Desalination and Water Treatment
www.deswater.com

doi: 10.5004/dwt.2018.23241

136 (2018) 31–38
December

Application of direct contact membrane distillation for treating high salinity solutions: impact of membrane structure and chemistry

Mustafa Al-Furaiji[a], Nieck Benes[b], Arian Nijmeijer[b], Jeffrey R. McCutcheon[c,*]

[a]*Environment and Water Directorate, Ministry of Science and Technology, Baghdad, Iraq, email: alfuraiji79@gmail.com*
[b]*Inorganic Membranes, Mesa+ Institute for Nanotechnology, University of Twente, P.O. Box 217 7500, AE Enschede, The Netherlands, emails: n.e.benes@utwente.nl (N. Benes), a.nijmeijer@utwente.nl (A. Nijmeijer)*
[c]*Department of Chemical and Biomolecular Engineering, University of Connecticut, 191 Auditorium Rd. Unit 3222, Storrs, CT 06269-3222, USA, email: jeff@engr.uconn.edu*

Received 11 August 2018; Accepted 3 October 2018

ABSTRACT

In this work, we examine membranes consisting of different materials, different pore sizes and thicknesses. The objective is to elucidate structural- and chemical-property relationships of direct contact membrane distillation for brine concentration using three different salts ($MgCl_2$, KCl, or NaCl) at near saturation conditions (up to 4 M). All membranes show excellent performance (high water flux and salt rejection above 99.5% for each salt). In general, the thinnest membranes exhibit the highest flux while lower porosity membranes have lower flux. Pore size is shown to have only a modest impact on performance. Solutes will also play an important role in MD water flux.

Keywords: Membrane distillation; Brine; ECTFE membrane; PVDF membrane; PP membrane

1. Introduction

There are few membrane technologies available today that can dewater or treat high salinity and high concentration solutions [1]. High osmotic pressures typically limit conventional processes such as reverse osmosis and high electricity costs are prohibitive when considering electro dialysis. Evaporative techniques are the most conventional approach to dewatering brines. Tall, cumbersome distillation columns and evaporators that are subject to corrosion in high salinity environments create their own obstacles, however [2].

Membrane distillation (MD) is an evaporative technique that employs a polymer membrane to moderate the evaporative interface. Using non-wetting polymeric membranes allows the tailoring of the interface at low cost while avoiding corrosion issues. These benefits have led to a bevy of literature on MD [3–6] for a variety of applications involving high salinity brines. Applications include oil and gas production wastewater, industrial wastewaters, and mining wastes.

There are numerous options for operating MD. Many academic studies have considered direct contact membrane distillation (DCMD) given its relative simplicity. However, DCMD has its drawbacks. The use of hydrophobic membranes makes these membranes prone to fouling (a problem in any MD process). Therefore, DCMD has largely been limited to use with "pristine" brines. Pristine brines can be created by extensive pretreatment or they may be present by design in certain processes (such as draw solutions for forward osmosis process). MD has been considered more viable when coupled with another process, such as forward osmosis (FO). In such FO–MD systems, FO acts as a pretreatment for the MD system, removing essentially all foulants, while the MD concentrates the brine that serves as the draw solution for FO. The use of MD in FO systems has been of particular interest recently [7–9] and necessitates testing performance using very high salinity brines. Only a few studies are published examining DCMD performance with brines [10,11] and these studies do not evaluate a large number of membranes.

* Corresponding author.

DCMD performance of high salinity brines must be tested across a wide spectrum of membranes with different properties that may impact performance. Pore size, thickness, and membrane chemistry are all critical features of membranes that will change flux and rejection; however, the literature lacks a systematic investigation of these structure- and chemistry-performance relationships. There has been limited work in studying pore size in DCMD [6,12] and air gap membrane distillation [13], but there is no systematic study on how different membrane features may change performance due to mass transfer resistance or heat transfer.

In this paper, the impact of membrane properties and brine solution type on DCMD performance (flux, selectivity) in treatment of highly concentrated solutions is investigated. Included in this study is the performance of previously untested membranes from 3M made from ethylene chlorotrifluoroethylene (ECTFE). All of the tested membranes exhibited excellent selectivity for a variety of salts (near 100% rejection). Substantial difference in water flux is observed for different membranes and salt type. In all, for the size of membranes tested in this study, thinner membranes are preferable as they exhibit lower mass transfer resistance. Heat transfer is of less importance when testing at this coupon size. However, at large scale, energy efficiency is of more importance.

2. Materials and methods

2.1. Materials

Sodium chloride (NaCl), potassium chloride (KCl), and magnesium chloride hexahydrate ($MgCl_2 \cdot 6H_2O$) were analytical reagents purchased from Fisher Scientific (Pittsburgh, PA). The PVDF-HVHP microporous flat sheet membrane (0.45 μm pore size) was purchased from Millipore (Kankakee, IL). The ECTFE membrane (pore size 0.45 μm) was provided by 3 M. PP membranes with different pore sizes (0.45, 0.2 and 0.1 μm) were acquired from 3 M. Detailed characterization of the membranes used in this research is provided in Table 1.

2.2. Membrane characterization

The surface of the different membranes was examined by scanning electron microscopy (SEM) using a cold cathode field emission scanning electron microscope JSM-6335F (FESEM, JEOL Ltd., Japan). Prior to imaging, the samples were sputter coated with a thin layer of gold. Imaging was done using an accelerating voltage of 10 kV and current of 12 μA. A CAM 101 series contact angle goniometer was used to measure the contact angles of the membranes at five different locations for each sample. The thickness of the membranes was measured at no less than five different locations of the membrane using digital micrometer (series 293 IP65, Mitutoyo, Aurora, IL).

2.3. Membrane distillation test protocol

The DCMD tests were carried out using the experimental set-up shown in Fig. 1. The installation consists of two tanks: one for the feed solution and the other for permeate. Feed solution and permeate were pumped to the membrane cell using variable speed peristaltic pumps from Cole-Parmer (Vernon Hills, IL). A detailed description with pictures of the membrane cell, a plate and frame membrane contactor, is given elsewhere [14]. The flow of the feed and permeate was controlled by flow meters and the pressure is monitored by pressure gauges on both lines. Four thermocouples, connected to a four-channel temperature controller from Sper Scientific Direct (Scottsdale, AZ), were used to measure the temperature at the inlets and the outlets of the membrane cell. The temperature of the feed solution was kept at 50°C using a heater (Fisher Scientific) while permeate was kept at 20°C using a chiller (Fisher Scientific).

The water flux was calculated based on the weight change of the collected permeate over the experiment time (6 h). The salt rejection (R) was calculated from the following equation:

$$R = \left(1 - \frac{C_p}{C_{f,i}}\right) \times 100\% \quad (1)$$

where C_{fi} (g/L) is the initial concentration of the solute in the feed solution, and C_p (g/L) is the solute concentration at the permeate calculated from:

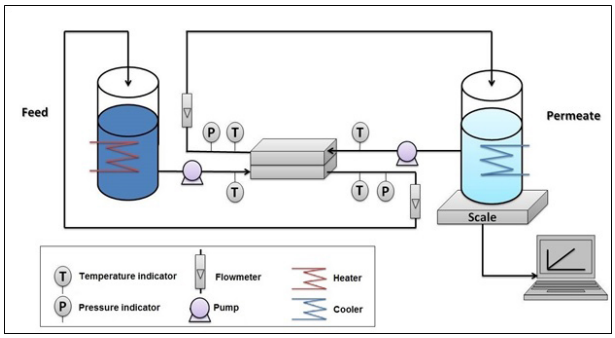

Fig. 1. Schematic diagram of the DCMD bench-scale test unit.

Table 1
Properties of membranes used in this study

	Manufacturer	Pore size (μm)[a]	Porosity (%)[a]	Thickness (μm)[b]	Contact angle[b]
0.45 PVDF	Millipore	0.45	66	105	115 ± 7
0.45 ECTFE	3M	0.45	81	50	103 ± 10
0.45 PP	3M	0.45	85	115	126 ± 7
0.2 PP	3M	0.2	85	114	130 ± 6
0.1 PP	3M	0.1	70	57	117 ± 5

[a]From the manufacturer.
[b]Our measurements.

$$C_p = \frac{C_{p,t}\left(V_{p,i} + \Delta V\right) - C_{p,i}V_{p,i}}{\Delta V} \quad (2)$$

In this equation $C_{p,i}$, and $C_{p,f}$ are the initial and final solute concentration at the permeate side, $V_{p,I}$ is the initial permeate volume and ΔV is the permeate volume change during the experiment. The concentration of the solute in the permeate tank was calculated from measuring the conductivity of permeate using an YSI 3200 conductivity meter. All experiments were run for a period of 6 h to evaluate wetting potential and stability of flux and selectivity.

3. Theory

3.1. Heat transfer

The temperature polarization coefficient (TPC) is used to quantify the difference between the temperatures on the membrane surfaces and that in the bulks of both the feed solution and permeate. A membrane with a higher TPC (for the same operation and hydrodynamic conditions) provides better insulation between the feed solution and permeate and consequently better performance (higher water flux). In order to calculate the temperature polarization coefficient, we used the equations.

$$\mathrm{TPC} = \frac{T_{\mathrm{fm}} - T_{\mathrm{pm}}}{T_f - T_p} \quad (3)$$

where T_f and T_p are the bulk temperatures of the feed solution and permeate, T_{fm}, T_{pm} are the temperature of the feed solution and permeate at the membrane surfaces and can be from the basic conduction and convection heat transfer equations:

$$h_f \times (T_f - T_{f,m}) = J \times \Delta H_v\left(T_{\mathrm{ave}}\right) + \frac{k_m \times \left(T_{f,m} - T_{p,m}\right)}{\delta_m} \quad (4)$$

$$h_p \times (T_{p,m} - T_p) = J \times \Delta H_v\left(T_{\mathrm{ave}}\right) + \frac{k_m \times \left(T_{f,m} - T_{p,m}\right)}{\delta_m} \quad (5)$$

where J is the water flux which was obtained from the experiment, $\Delta H_v(T_{\mathrm{ave}})$ is the latent heat of vaporization at the average temperature of the feed and permeate which can be calculated from the following equation [15]:

$$H_v\left(T\right) = 1.7535 \times T + 2024.3 \quad (6)$$

k_m is the thermal conductivity of the membrane which is expressed as [16]:

$$k_m = \varepsilon k_a + \left(1 - \varepsilon\right)k_p \quad (7)$$

where ε is the membrane porosity, k_a and k_p are the thermal conductivities of air and the polymer of the membrane, respectively.

Heat transfer coefficients on the feed solution and permeate sides (h_f and h_p) under laminar flow conditions can be calculated from the Nusselt number (Nu) correlation for laminar flow in rectangular channel [17]:

$$\mathrm{Nu} = 0.13\,\mathrm{Re}^{0.64}\,\mathrm{Pr}^{0.38} \quad (8)$$

where Re is the Reynolds number and Pr is the Prandtl number.

3.2. Mass transfer

The effective driving force for the mass (water vapor) transfer through the membrane is the difference between the vapor pressures of the feed and the permeate solution, at the membrane surface. The membrane distillation coefficient (MDC) can be used as an indicator of how well the membrane performs given the effective driving force.

The MDC in DCMD is calculated from the linear relation between the water flux and the driving force across the membrane [18]:

$$\mathrm{MDC} = \frac{J}{\left(p_{\mathrm{mf}} - p_{\mathrm{mp}}\right)} \quad (9)$$

where p_{mf} and p_{mp} are the partial pressures of the feed and permeate sides evaluated from temperatures at the membrane surfaces (T_{mf} and T_{mp}).

The mechanism of mass transfer in a microporous membrane can be determined from Knudsen number (K_n) which is the ratio between the mean free path (λ) and the pore size diameter (d_p) [15]:

$$K_n = \frac{\lambda}{d_p} \quad (10)$$

λ is calculated from the following expression [19]:

$$\lambda = \frac{k_B T}{\sqrt{2}\pi p_m \left(\sigma_m\right)^2} \quad (11)$$

where k_B is the Boltzmann constant (1.38×10^{-23} m^2 kg s^{-1} K^{-1}), T is the absolute temperature, p_m is the mean pressure within the membrane pores and σ_m is the collision diameter of water molecules (2.641 Å).

4. Results and discussion

4.1. Effect of membrane characteristics on the MD process

Table 1 shows the properties of the commercial membranes used in this study. It should be noted that the 3 M membranes have a higher porosity than the Millipore membrane. PP membranes exhibit higher contact angles due to their higher hydrophobicity. The 0.45 μm ECTFE and 0.1 PP membranes have thicknesses of about half than that of the other membranes. The morphology of the different

membrane materials is shown in Fig. 2. Each membrane has a nodular structure that provides surface roughness and regular pore size to prevent wetting.

4.1.1. Membrane material type

To compare the different membrane's performance in DCMD, we considered a single brine, 5 M NaCl, as a feed solution. This concentration was chosen to cover for the whole range of concentrations of the draw solutions that can be used for FO. It can be seen from Fig. 3 that 0.45 μm ECTFE membrane showed the highest flux. The polypropylene membrane exhibited statistically similar flux, but the 0.45 μm PVDF membrane exhibited less than half of the flux. This result is attributed to the difference in structural properties between the membranes. The ECTFE membrane is half as thick as the PVDF membrane. It has been reported that a thin membrane is favorable in MD as it poses less mass transport resistance [20]. Interestingly enough, the PP membrane is actually thicker than the PVDF, though it is reported to have a higher porosity as well. Membranes with higher porosity offer more surface for vapor generation [4] while at the same time have lower heat conduction through membrane. It is important to also note, however, that even though these membranes had different fluxes, all exhibited complete salt rejection during the 6 h test.

The thickness differences highlight an important tradeoff between mass transfer and thermal efficiency in MD. A thinner membrane generally yields higher fluxes because the membrane offers less resistance to the mass transfer. However, a thinner membrane shows higher heat loss due to conduction and thus more a severe temperature polarization effect. Fig. 4 shows the calculated values of the TPC and MDC for the different membranes. Even though the 0.45 μm ECTFE membrane shows the highest flux, it has the lowest TPC. However, the 0.45 μm ECTFE membrane has a higher MDC indicating its good mass transfer performance. It can be seen from Fig. 4 that the mass transfer (represented by MDC) is dominant over the heat transfer (represented by TPC).

4.1.2. Pore size effect

The effect of pore size on DCMD performance was investigated using 3M PP membranes with different pore sizes (i.e., 0.45, 0.2, and 0.1 μm). Fig. 5 shows that only small differences in water flux between the membranes and that these differences are statistically not significant (especially between the 0.45 μm and the 0.2 μm PP membranes). No difference in salt rejection was detected for the three membranes either. Theoretically, large pore size is favorable for a high water flux due to lower mass transport resistance, but the pores must always be small enough to prevent pore wetting [21]. Slight

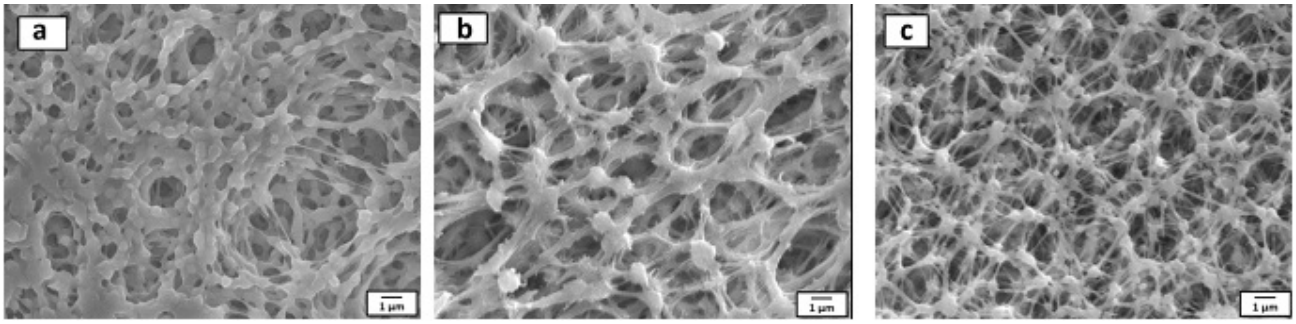

Fig. 2. SEM images of the different membrane materials used in this study. (a) 0.45 PVDF, (b) 0.45 ECTFE and (c) 0.45 PP.

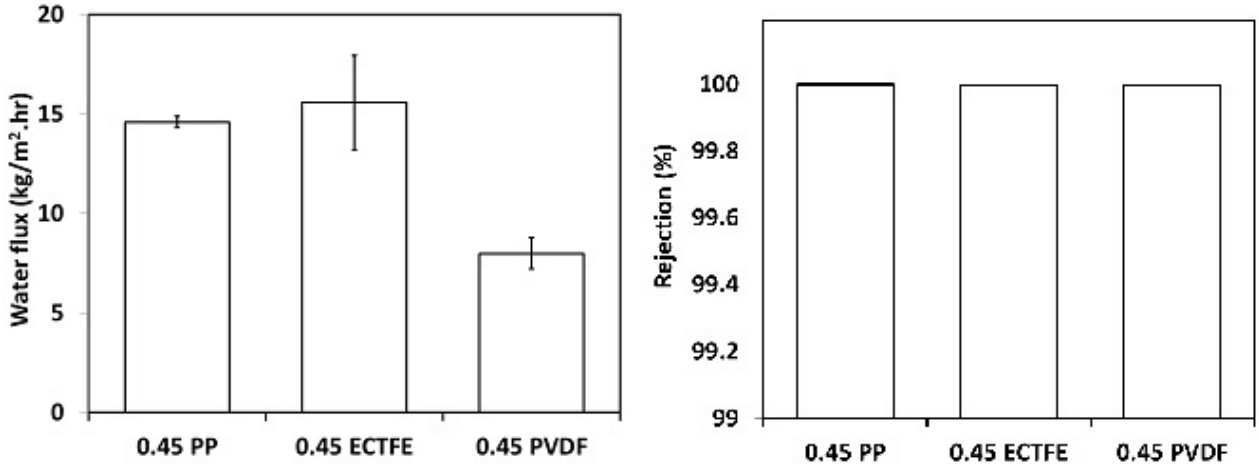

Fig. 3. Effect of membrane type on the water flux and the rejection. Experimental conditions: feed solution: 5 M NaCl, permeate: DI water, feed temperature: 50°C, permeate temperature: 20°C, cross-flow velocity of feed and permeate 0.25 m/s.

difference in the flux performances between the 0.1 μm PP membrane and the other two membranes could be attributed to the porosity and thickness differences (membranes that only differed in pore size were unfortunately not available). The thin 0.1 μm pore size membrane had a more severe TPC but had a higher MDC (Fig. 6). These trends match those found in Fig. 4.

Based on the Knudsen number (Table 2) the dominant mechanism of mass transfer for the 0.1 μm PP membrane is Knudsen diffusion, implying that the diffusing molecules

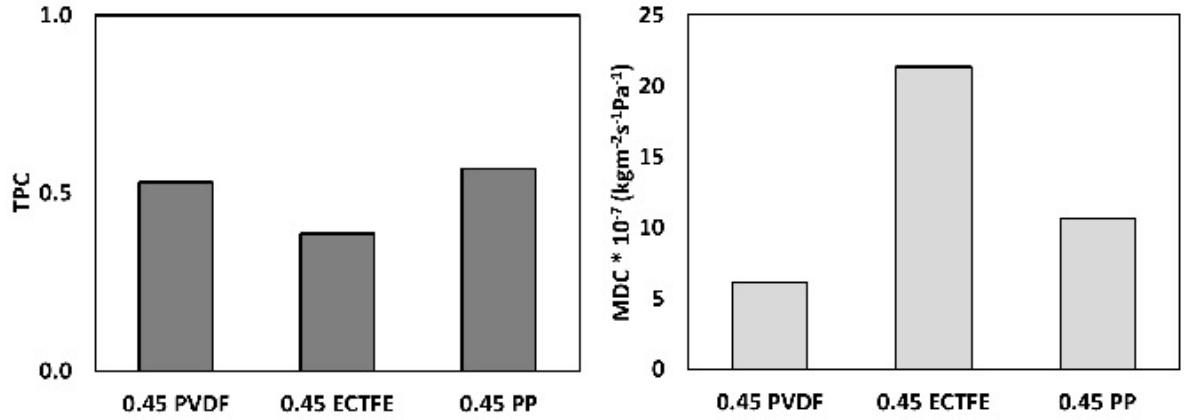

Fig. 4. *i* and MDC for the different membranes.

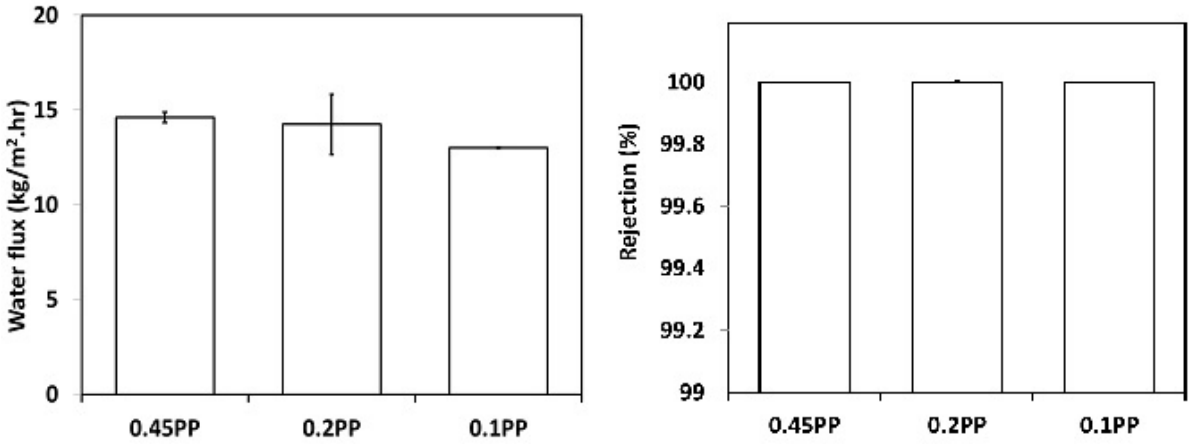

Fig. 5. Effect of pore size on the water flux and the rejection. Experimental conditions: feed solution: 5 M NaCl, permeate: DI water, feed temperature: 50°C, permeate temperature: 20°C, cross-flow velocity of feed and permeate 0.25 m/s.

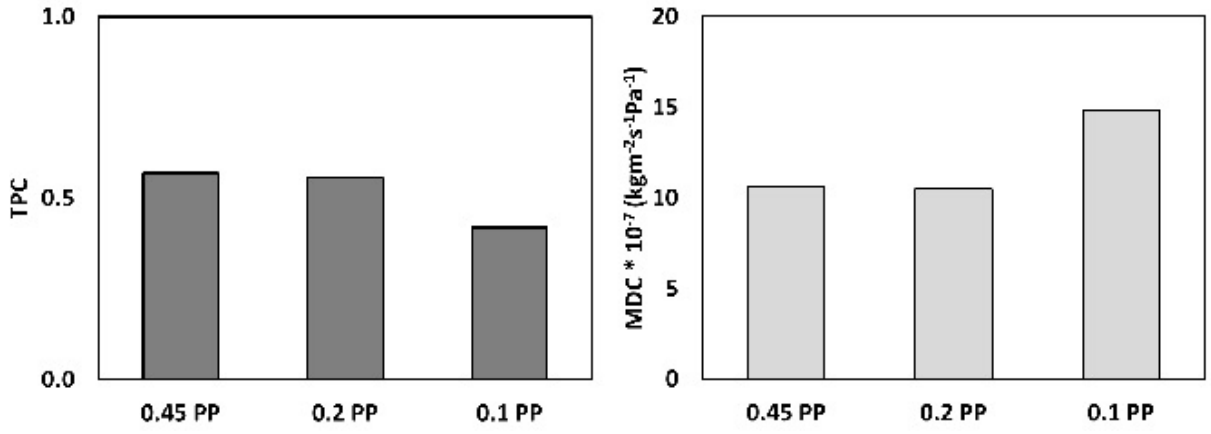

Fig. 6. TPC and MDC for the PP membrane at different pore sizes.

collide with the walls of the pores much more frequently than they collide with other molecules [22]. For the 0.45 μm and the 0.2 μm membranes the contribution of molecular diffusion to transport is slightly larger. The additional friction on the permeating water, associated with molecular diffusion, can result in an increased overall resistance to mass transfer [23,24]; the faster mass transfer due to a larger pore size may be negatively outweighed by the additional resistance associated with the molecular diffusion. This could explain the lower calculated MDC values observed for the larger pore size membranes (Fig. 6).

4.2. Effect of salt type

Fig. 7 shows the water flux vs. time data of the 0.45 PP membrane, for three different highly concentrated (4 M) salt solutions. The KCl solution shows the highest water flux, followed by the NaCl solution. For $MgCl_2$, relatively low flux is observed. For better manifestation of the flux data, we present in Fig. 8 the average water flux and the salt rejection for the different feed solutions. For all three solutions, a salt rejection >99.9% is observed. The differences in the fluxes are caused by the differences in vapor pressure of the different solutions. Fig. 9 shows the vapor pressure of the solutions at 50°C, over a range of concentrations. At 4 M concentration, the vapor pressure of $MgCl_2$ is lower than that of NaCl and KCl. The low vapor pressure of the $MgCl_2$ solution explains its lower water flux. Furthermore, the viscosity of the $MgCl_2$ solution is much higher (6.2 cP) than the viscosity of NaCl (1.37 cP) and KCl (1.07 cP) solutions. Higher viscosity increases the resistance to the mass and heat transfer in the feed solution boundary layer [10,11].

Table 2
Knudsen number for the different PP membranes

Membrane	K_n	Mechanism
0.45 PP	0.32	Combined
0.2 PP	0.71	Combined
0.1 PP	1.42	Knudsen

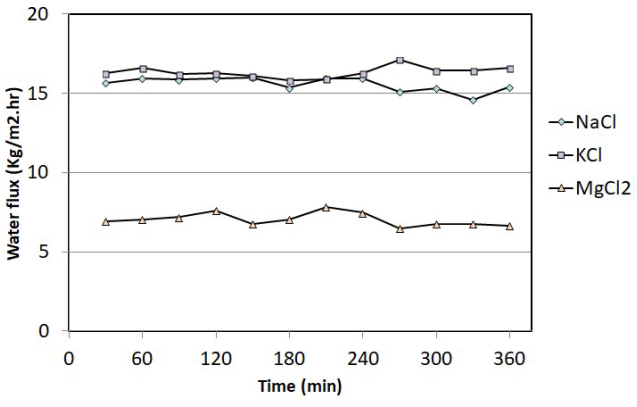

Fig. 7. Effect of salt type on the water flux. Experimental conditions: 0.45 PP membrane, permeate: DI water, feed temperature: 50°C, permeate temperature: 20°C, cross-flow velocity of feed and permeate 0.25 m/s.

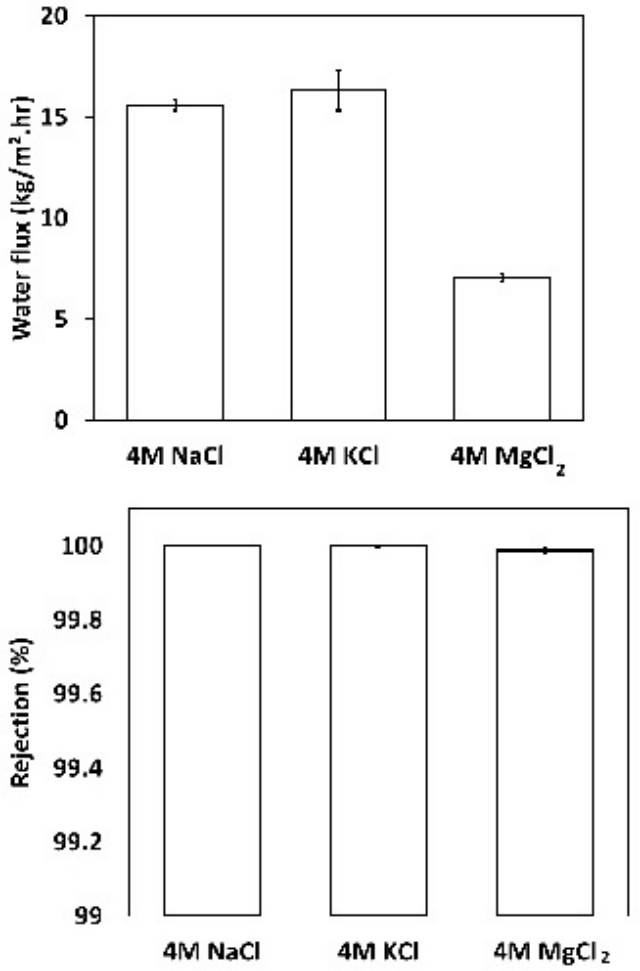

Fig. 8. Effect of salt type on the average water flux and the salt rejection. Experimental conditions: 0.45 PP membrane, permeate: DI water, feed temperature: 50°C, permeate temperature: 20°C, cross-flow velocity of feed and permeate 0.25 m/s.

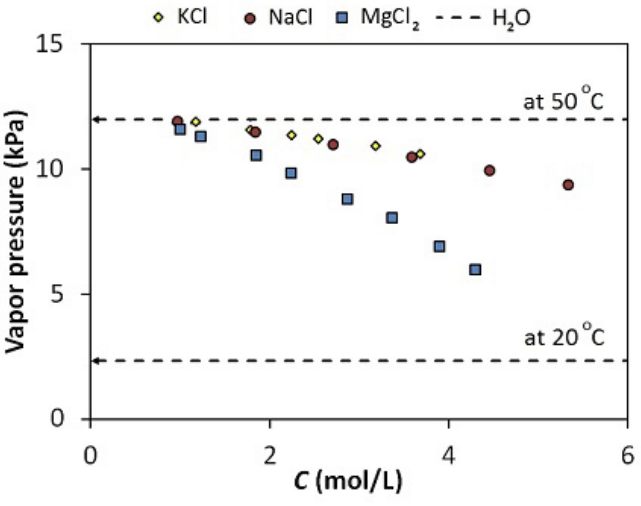

Fig. 9. Vapor pressure of the different salts at 50°C [25–27].

5. Conclusions

This systematic study demonstrated that certain structural characteristics of commercial membranes, in particular their thickness, contribute to substantial differences in their flux performance in DCMD. The data suggest that reducing the thickness of a membrane results in a complex interplay between reduced mass transfer resistance and enhanced for heat transfer. In most membrane processes, reducing mass transfer resistance without sacrificing selectivity is of paramount importance. However, in applications such as DCMD, lower mass transfer resistance may lead to higher heat flux, which lowers overall driving force. The calculated values of TPC and MDC for the membranes with different thicknesses confirmed that mass transfer is more predominant than heat transfer. Interestingly, pore size was shown to have only limited impact on DCMD performance over the range of pore sizes measured even though it substantially impacts resistance in pressure driven systems. Strikingly, even for highly concentrated solutions, the salt rejections are near 100%. The results also suggest that DCMD can be promising option for hybridization with FO where retention of the draw solute is critical to system performance. Lastly, the ECTFE membranes, which have yet to be reported on, performed quite well during our testing suggesting their utility for DCMD applications.

Acknowledgments

The authors would like to acknowledge funding from the higher committee for education development (HCED) in Iraq. The authors would also like to thank 3M for providing ECTFE and PP membranes for this work.

Symbols

$C_{f,I}$	—	Initial concentration of the solute in the feed solution, g L^{-1}
C_p	—	Solute concentration at the permeate, g L^{-1}
$C_{p,f}$	—	Final solute concentration at the permeate side, g L^{-1}
$C_{p,I}$	—	Initial solute concentration at the permeate side, g L^{-1}
d_p	—	Pore diameter, μm
ECTFE	—	Ethylene chloro trifluoroethylene
h_f	—	Heat transfer coefficient of the feed side, W m^{-2} K^{-1}
h_p	—	Heat transfer coefficient of the permeate side W m^{-2} K^{-1}
J	—	Mass flux, kg m^{-2} h^{-1}
k_a	—	Thermal conductivity of air, W m^{-1} K^{-1}
k_B	—	Boltzmann constant, $1.38*10^{-23}$ kg m^2 s^{-1} K^{-1}
k_m	—	Thermal conductivity of membrane, W m^{-1} K^{-1}
k_p	—	Thermal conductivity of polymer, W m^{-1} K^{-1}
M	—	Molecular weight of water, kg mol^{-1}
MDC	—	MD coefficient, kg m^{-2} s^{-1} Pa^{-1}
Nu	—	Nusselt number
p_m	—	Mean pressure within the membrane pores, Pa
p_{mf}	—	Partial pressure of water at the feed side, Pa
p_{mp}	—	Partial pressure of water at the permeate side, Pa
PP	—	Polypropylene
Pr	—	Prandtl number
PVDF	—	Polyvinylidene fluoride
R	—	Salt rejection
Re	—	Reynolds number
T_f	—	Bulk temperature of the feed side, K
$T_{f,m}$	—	Membrane surface temperature at the feed side, K
T_p	—	Bulk temperature of the permeate side, K
$T_{p,m}$	—	Membrane surface temperature at the permeate side, K
TPC	—	Temperature polarization coefficient
$V_{p,I}$	—	Initial permeate volume, L
δ_m	—	Membrane thickness, μm
ΔH_v	—	Latent heat of vaporization, kJ kg^{-1}
λ	—	Mean free path, nm
σ_w	—	Collision diameter of water molecule, 2.641 Å

References

[1] D.L. Shaffer, L.H. Arias Chavez, M. Ben-Sasson, S. Romero-Vargas Castrillón, N.Y. Yip, M. Elimelech, Desalination and reuse of high-salinity shale gas produced water: drivers, technologies, and future directions, Environ. Sci. Technol., 47 (2013) 9569–9583.

[2] S. Vigneswaran, Ed., Waste Water Treatment Technologies - Volume III, Encyclopedia of Life Support Systems (EOLSS), 2009.

[3] K. Lawson, Membrane distillation, J. Membr. Sci., 124 (1997) 297–369.

[4] E. Curcio, E. Drioli, Membrane distillation and related operations—a review, Sep. Purif. Rev., 34 (2005) 35–86.

[5] E. Drioli, A. Ali, F. Macedonio, Membrane distillation: recent developments and perspectives, Desalination, 356 (2015) 56–84.

[6] A. Alkhudhiri, N. Darwish, N. Hilal, Membrane distillation: a comprehensive review, Desalination, 287 (2012) 2–18.

[7] S. Zhang, P. Wang, X. Fu, T.-S. Chung, Sustainable water recovery from oily wastewater via forward osmosis-membrane distillation (FO-MD), Water Res., 52 (2014) 112–121.

[8] Q. Ge, P. Wang, C. Wan, T.-S. Chung, Polyelectrolyte-promoted forward osmosis–membrane distillation (FO–MD) hybrid process for dye wastewater treatment, Environ. Sci. Technol., 46 (2012) 6236–6243.

[9] M. Xie, L.D. Nghiem, W.E. Price, M. Elimelech, S. Water, N. Haven, Toward resource recovery from wastewater: extraction of phosphorus from digested sludge using a hybrid forward osmosis–membrane distillation process, Environ. Sci. Technol. Lett., 1 (2014) 191–195.

[10] J. Li, Y. Guan, F. Cheng, Y. Liu, Treatment of high salinity brines by direct contact membrane distillation: effect of membrane characteristics and salinity, Chemosphere, 140 (2015) 143–149.

[11] Y. Guan, J. Li, F. Cheng, J. Zhao, X. Wang, Influence of salt concentration on DCMD performance for treatment of highly concentrated NaCl, KCl, $MgCl_2$ and $MgSO_4$ solutions, Desalination, 355 (2015) 110–117.

[12] M.S. El-Bourawi, Z. Ding, R. Ma, M. Khayet, A framework for better understanding membrane distillation separation process, J. Membr. Sci., 285 (2006) 4–29.

[13] A. Alkhudhiri, N. Darwish, N. Hilal, Treatment of high salinity solutions: application of air gap membrane distillation, Desalination, 287 (2012) 55–60.

[14] D. Anastasio, J.R. McCutcheon, Using forward osmosis to teach mass transfer fundamentals to undergraduate chemical engineering students, Desalination, 312 (2013) 10–18.

[15] P. Termpiyakul, R. Jiraratananon, S. Srisurichan, Heat and mass transfer characteristics of a direct contact membrane distillation process for desalination, Desalination, 177 (2005) 133–141.

[16] J. Phattaranawik, R. Jiraratananon, A. Fane, Heat transport and membrane distillation coefficients in direct contact membrane distillation, J. Membr. Sci., 212 (2003) 177–193.

[17] M. Gryta, M. Tomaszewska, A. Morawski, Membrane distillation with laminar flow, Sep. Purif. Technol., 11 (1997) 93–101.
[18] M. Qtaishat, T. Matsuura, B. Kruczek, M. Khayet, Heat and mass transfer analysis in direct contact membrane distillation, Desalination, 219 (2008) 272–292.
[19] M. Khayet, T. Matsuura, Membrane Distillation: principles and applications, Elsevier, Amsterdam, The Netherlands, 2011.
[20] M. Essalhi, M. Khayet, Self-sustained webs of polyvinylidene fluoride electrospun nanofibers at different electrospinning times: 1. Desalination by direct contact membrane distillation, J. Membr. Sci., 433 (2013) 167–179.
[21] K.W. Lawson, D.R. Lloyd, Membrane distillation, J. Membr. Sci., 124 (1997) 1–25.
[22] E. Cussler, Diffusion: Mass Transfer in Fluid Systems, 3rd ed., Cambridge University Press, New York, USA, 2009.
[23] M. Khayet, T. Matsuura, J.I. Mengual, Porous hydrophobic/hydrophilic composite membranes: estimation of the hydrophobic-layer thickness, J. Membr. Sci., 266 (2005) 68–79.
[24] S. Adnan, M. Hoang, H. Wang, Z. Xie, Commercial PTFE membranes for membrane distillation application: effect of microstructure and support material, Desalination, 284 (2012) 297–308.
[25] E.C.W. Clarke, D.N. Glew, Evaluation of the thermodynamics functions for aqueous sodium chloride from equilibrium and calorimetric measurements below 154C, J. Phys. Chem. Ref. Data, 14 (1985) 489–610.
[26] D.W. Green, R.H. Perry, Perry's Chemical Engineers' Handbook, 8th ed., McGraw-Hill, New York, 2008.
[27] K.R. Patil, A.D. Tripathi, G. Pathak, S.S. Katti, Thermodynamic properties of aqueous electrolyte solutions. 2. Vapor pressure of aqueous solutions of sodium bromide, sodium iodide, potassium chloride, potassium bromide, potassium iodide, rubidium chloride, cesium chloride, cesium bromide, cesium iodide, J. Chem. Eng. Data, 36 (1991) 225–230.